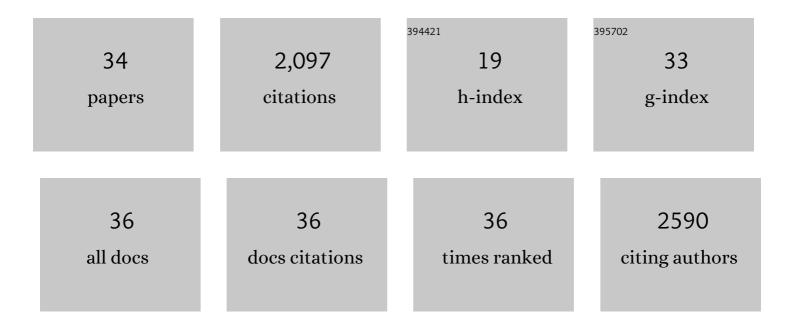
Boris Keil

List of Publications by Year in descending order

Source: https://exaly.com/author-pdf/7566730/publications.pdf Version: 2024-02-01



RODIS KEII

#	Article	IF	CITATIONS
1	A 31 hannel integrated "AC/DC―B ₀ shim and radiofrequency receive array coil for improved 7T MRI. Magnetic Resonance in Medicine, 2022, 87, 1074-1092.	3.0	14
2	Selective responses to faces, scenes, and bodies in the ventral visual pathway of infants. Current Biology, 2022, 32, 265-274.e5.	3.9	43
3	Comprehensive diffusion MRI dataset for in vivo human brain microstructure mapping using 300 mT/m gradients. Scientific Data, 2022, 9, 7.	5.3	16
4	Mapping the human connectome using diffusion MRI at 300 mT/m gradient strength: Methodological advances and scientific impact. NeuroImage, 2022, 254, 118958.	4.2	18
5	A patientâ€friendly 16 hannel transmit/64 hannel receive coil array for combined head–neck MRI at 7 Tesla. Magnetic Resonance in Medicine, 2022, 88, 1419-1433.	3.0	13
6	In vivo human whole-brain Connectom diffusion MRI dataset at 760 µm isotropic resolution. Scientific Data, 2021, 8, 122.	5.3	37
7	A sizeâ€adaptive 32â€channel array coil for awake infant neuroimaging at 3ÂTesla MRI. Magnetic Resonance in Medicine, 2021, 86, 1773-1785.	3.0	11
8	Optimized 64•hannel array configurations for accelerated simultaneous multislice acquisitions in 3T cardiac MRI. Magnetic Resonance in Medicine, 2021, 86, 2276-2289.	3.0	7
9	A 48-channel receive array coil for mesoscopic diffusion-weighted MRI of exÂvivo human brain on the 3 T connectome scanner. Neurolmage, 2021, 238, 118256.	4.2	13
10	Connectome 2.0: Developing the next-generation ultra-high gradient strength human MRI scanner for bridging studies of the micro-, meso- and macro-connectome. NeuroImage, 2021, 243, 118530.	4.2	58
11	Ultra-high field (7T) functional magnetic resonance imaging in amyotrophic lateral sclerosis: a pilot study. NeuroImage: Clinical, 2021, 30, 102648.	2.7	10
12	Response patterns in the developing social brain are organized by social and emotion features and disrupted in children diagnosed with autism spectrum disorder. Cortex, 2020, 125, 12-29.	2.4	9
13	Representational similarity precedes category selectivity in the developing ventral visual pathway. NeuroImage, 2019, 197, 565-574.	4.2	29
14	Feasibility of using linearly polarized rotating birdcage transmitters and close-fitting receive arrays in MRI to reduce SAR in the vicinity of deep brain simulation implants. Magnetic Resonance in Medicine, 2017, 77, 1701-1712.	3.0	70
15	Organization of high-level visual cortex in human infants. Nature Communications, 2017, 8, 13995.	12.8	224
16	Construction and modeling of a reconfigurable MRI coil for lowering SAR in patients with deep brain stimulation implants. NeuroImage, 2017, 147, 577-588.	4.2	58
17	Ultra high-field (7tesla) magnetic resonance spectroscopy in Amyotrophic Lateral Sclerosis. PLoS ONE, 2017, 12, e0177680.	2.5	45
18	A 32-Channel Head Coil Array with Circularly Symmetric Geometry for Accelerated Human Brain Imaging. PLoS ONE, 2016, 11, e0149446.	2.5	3

BORIS KEIL

#	Article	IF	CITATIONS
19	General design approach and practical realization of decoupling matrices for parallel transmission coils. Magnetic Resonance in Medicine, 2016, 76, 329-339.	3.0	8
20	Coilâ€ŧo oil physiological noise correlations and their impact on functional MRI timeâ€series signalâ€ŧoâ€noise ratio. Magnetic Resonance in Medicine, 2016, 76, 1708-1719.	3.0	21
21	Intracortical depth analyses of frequency-sensitive regions of human auditory cortex using 7T fMRI. NeuroImage, 2016, 143, 116-127.	4.2	46
22	A 32 hannel combined RF and <i>B₀</i> shim array for 3T brain imaging. Magnetic Resonance in Medicine, 2016, 75, 441-451.	3.0	106
23	Dense, shapeâ€optimized posterior 32â€channel coil for submillimeter functional imaging of visual cortex at 3T. Magnetic Resonance in Medicine, 2016, 76, 321-328.	3.0	10
24	MGH–USC Human Connectome Project datasets with ultra-high b-value diffusion MRI. NeuroImage, 2016, 124, 1108-1114.	4.2	209
25	A 31â€channel MR brain array coil compatible with positron emission tomography. Magnetic Resonance in Medicine, 2015, 73, 2363-2375.	3.0	38
26	In vivo mapping of human spinal cord microstructure at 300 mT/m. NeuroImage, 2015, 118, 494-507.	4.2	69
27	Nineteen-channel receive array and four-channel transmit array coil for cervical spinal cord imaging at 7T. Magnetic Resonance in Medicine, 2014, 72, spcone-spcone.	3.0	0
28	Investigating the Capability to Resolve Complex White Matter Structures with High <i>b</i> -Value Diffusion Magnetic Resonance Imaging on the MGH-USC Connectom Scanner. Brain Connectivity, 2014, 4, 718-726.	1.7	53
29	Nineteen-channel receive array and four-channel transmit array coil for cervical spinal cord imaging at 7T. Magnetic Resonance in Medicine, 2014, 72, 291-300.	3.0	52
30	Cortical Localization of Microbleeds in Cerebral Amyloid Angiopathy: An Ultra High-Field 7T MRI Study. Journal of Alzheimer's Disease, 2014, 43, 1325-1330.	2.6	35
31	A 64â€channel 3T array coil for accelerated brain MRI. Magnetic Resonance in Medicine, 2013, 70, 248-258.	3.0	202
32	Massively parallel MRI detector arrays. Journal of Magnetic Resonance, 2013, 229, 75-89.	2.1	143
33	The Human Connectome Project and beyond: Initial applications of 300mT/m gradients. NeuroImage, 2013, 80, 234-245.	4.2	309
34	Sizeâ€optimized 32â€channel brain arrays for 3 T pediatric imaging. Magnetic Resonance in Medicine, 2011, 66, 1777-1787.	3.0	118